21. The ground-based observations of the 15 November 1991 flare were obtained at the Mees Solar Observatory of the University of Hawaii.
22. R. S. Canfield *et al.*, *Publ. Astron. Soc. Jpn.*, in press.
23. T. Sakao *et al.*, *ibid.*, in press.
24. R. M. Winglee, A. L. Kiplinger, D. M. Zarro, G. A. Dulk, J. R. Lemen, *Appl. J.* **375**, 366 (1991).
25. K. Matsushita, S. Masuda, T. Kosugi, M. Inda, K. Yaji, *Publ. Astron. Soc. Jpn.*, in press.
26. A set of 33 papers presenting the first scientific results from Yohkoh are to appear in *Publ. Astron. Soc. Jpn.*, in press.
27. M. Akioka, H. Hudson, L. Acton *et al.*, in preparation.
28. S. Tsuneta *et al.*, *Publ. Astron. Soc. Jpn.*, in press.
29. L. W. Acton *et al.*, *ibid.*, in press.
30. J. Aboudarham and J. C. Henoux, *Solar Phys.* **121**, 19 (1989).
31. Y. Uchida *et al.*, *Publ. Astron. Soc. Jpn.*, in press.
32. K. Shibata *et al.*, *ibid.*, in press.
33. S. Tsuneta *et al.*, *ibid.*, in press.
34. K. Strong *et al.*, *ibid.*, in press.
35. In this period of difficult choices in space research it is worth noting some of the elements that have contributed to the success of Yohkoh. The composition of the Solar-A payload was determined by consensus within a small scientific community in Japan, resulting in the very effective use of limited resources. Launch slippage was not permitted, forcing the early resolution of technical and resource issues by the scientists who were responsible for, and in control of, the program. The science team was led by individuals experienced in space research and who were personally involved on a day-to-day basis from beginning to end. Finally, early preparation for data analysis, coupled with the computing power of modern workstations, have allowed effective access to the data from the time of launch.
36. We are grateful to the many colleagues and contractors whose labors brought the Yohkoh mission to fruition. Their names, too numerous to list here, may be found in references (*3*–*7*). We thank P. Martens and P. Sturrock for contributions to the manuscript and K. Strong, D. T. Roethig, A. McAllister, and G. Linford for assistance with the illustrations. The SXT program in the United States has been supported by NASA Marshall Space Flight Center under contract NAS8 37334 and the Lockheed Independent Research Program.

Seismic Tomogram of the Earth's Mantle: Geodynamic Implications

Yoshio Fukao

Recent seismic tomography of the Earth's mantle has revealed a large-scale pattern of mantle convection comprising upwelling columnar plumes in the Pacific and Africa and downwelling planar sheets along the Circum Pacific. Upwelling and downwelling occur most extensively under the south Pacific and west Pacific, respectively. High-resolution image of plate subduction has been obtained from the dense seismic networks around Japan. Japanese seismologists are in the best position to resolve the internal structure of downwelling current as an integral part of the whole convection system.

Tomogram is a combination of two Greek words, tomos (slice) and gramma (thing written), meaning reconstructed image of a body from projection. Tomography has been popularized by the physician's CT (computerized tomography) scanner. Images of cross sections of a human body are produced by measuring the attenuation of x-rays along a large number of lines through the cross section. Seismic tomography makes a similar image reconstruction for the Earth with the use of seismic waves, but there are many differences as well.

The first result of seismic tomography was reported by Aki and others (*1*) in 1974, who opened a window to go beyond the classic one-dimensional model of Earth's interior to search for a three-dimensional image. Hirahara's work (*2*) is an early example of an application of seismic tomography to the Japanese islands. Global-scale tomography has been pioneered by Dziewonski (*3*) and Woodhouse and Dziewonski (*4*). The physical parameters dealt with most often and determined most accurately in seismic tomography are compressional and shear wave velocities (*3*, *4*). The result is usually given in the form of deviation from the laterally averaged profile of the Earth because most of the variation in seismic velocity is due to the increase in hydrostatic pressure with depth. Lateral heterogeneity in seismic velocity is thought to be mostly the result of lateral temperature variation (high temperatures mean lower seismic velocities). Seismic tomography thus carries information about the solid-state convection in the mantle driven by internal radiogenic heat sources and heat conducted from the outer core (*5*). Plate tectonics provides a sinematic description of this convection only in the upper 100 km, where oceanic lithosphere forms at mid-oceanic-ridges, spreads, and is subducted beneath island arcs.

The deeper structure of mantle convection remains uncertain. The most controversial issue is the role of the seismic discontinuity at a depth of 660 km between the upper and lower mantle. Termination of earthquake activity at this depth has been interpreted as evidence that subducted oceanic lithosphere is prevented from sinking into the lower mantle across the 660-km discontinuity and has led to the idea that the convection associated with plate tectonics is restricted in the upper mantle (*6*). Recent seismic tomography has demonstrated conclusively that convection also occurs in the lower mantle (*7*, *8*). The upper and lower mantle thus convect with an unknown amount of mass exchanged between the upper and lower mantle. In this article, I review some of the seismic images of mantle convection to show that downwelling is occurring most intensely in the west Pacific including Japan. With this tectonic setting in mind, I discuss some of the strategies needed for future progress.

Seismic Tomogram of the Mantle

The most important difference of seismic tomography from medical tomography is the lack of design control over sources and receivers. In seismic tomography (excluding exploration geophysics) sources are natural earthquakes, the times and locations of which are out of our control. Their occurrence is spatially very uneven, limited largely to plate boundaries. Sensors are mostly placed on land and, even there, the locations are heavily dependent upon cultural and political factors. Seismic ray paths connecting source and receiver are, therefore, not evenly distributed within the mantle: some parts could be sampled by many ray paths but other parts may not. Fine parameterization of the whole mantle compatible with the well-sampled parts requires an excessively large number of model parameters. Coarse parameterization, on the other hand, loses some of the fundamental features that could be otherwise resolved. Tomography on a regional scale realizes fine parameterization by limiting the parameterized space to the well sampled part. The tomographic work by Hasegawa and co-workers represents the best example of this line of approach (*9*); they took advantage of a dense regional network and the occurrence of many shallow to deep earthquakes within the network to obtain the deep structure of the Northern Honshu arc. A similar approach has also been undertaken in other parts of Japan (*10*). The depth and horizontal extents of the model space (parameterized space) in this approach are strongly limited by the network configuration and hypocentral distribution. In order to further expand the model space, teleseismic events and arrival time data have often been incorporated (*11*, *12*). Incorporation of such data, however, brings another difficulty because, before inversion,

The author is in the Department of Earth and Planetary Sciences, Nagoya University, Chikusa, Nagoya 464-01, Japan.

the data have to be corrected for the travel of the waves through parts of the Earth outside the model.

Another approach, essentially a hybrid of regional-scale and global-scale tomography, is to make a fine parameterization for the well-sampled part and a coarse parameterization for the remaining part of the mantle; in this approach a good resolution can be achieved with a feasible number of model parameters, yet the difficulty of correction for teleseismic data can be avoided. Specifically the whole mantle is discretized into blocks such that the block size is smaller in a particular region sampled by many ray paths. For example, Fukao *et al.* (*13*) did such fine discretization beneath the west Pacific, where three major oceanic plates, the Pacific, Indian, and Philippine plates, are subducted into the mantle. The main purpose of this discretization was to image the trajectory of subducted slabs beyond the seismicity cutoff so as to resolve the fate of oceanic lithosphere. The data used were the first arrival times reported to the International Seismological Center (ISC) during the period 1976 to 1985 for about 4600 earthquakes including deep shocks. The total number of ray paths was about 420,000. The compressional wave velocity of about 56,000 blocks of the mantle was determined. The relation between the data and model parameters is nonlinear so that equation was solved iteratively, including an alternate step of relocation of all the events with a correction for the three-dimensional velocity perturbation

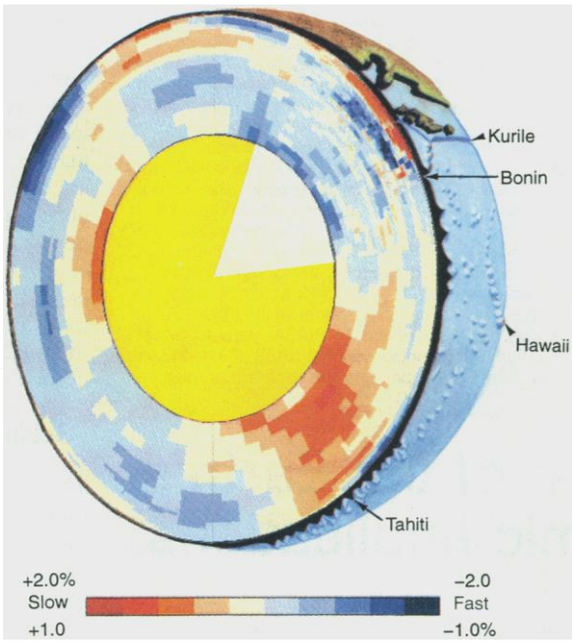

Fig. 1. A cross section of seismic velocity perturbations in the mantle (fast anomaly in blue and slow anomaly in red) along the great circle with a pole at (50°N, 90°W). The central part colored yellow (partly uncolored) corresponds to the Earth's core. This is a composite diagram of the unsmoothed section with a scale of ±2% (uncolored section at the center), and the smoothed section with a scale of ±1% (yellow section).

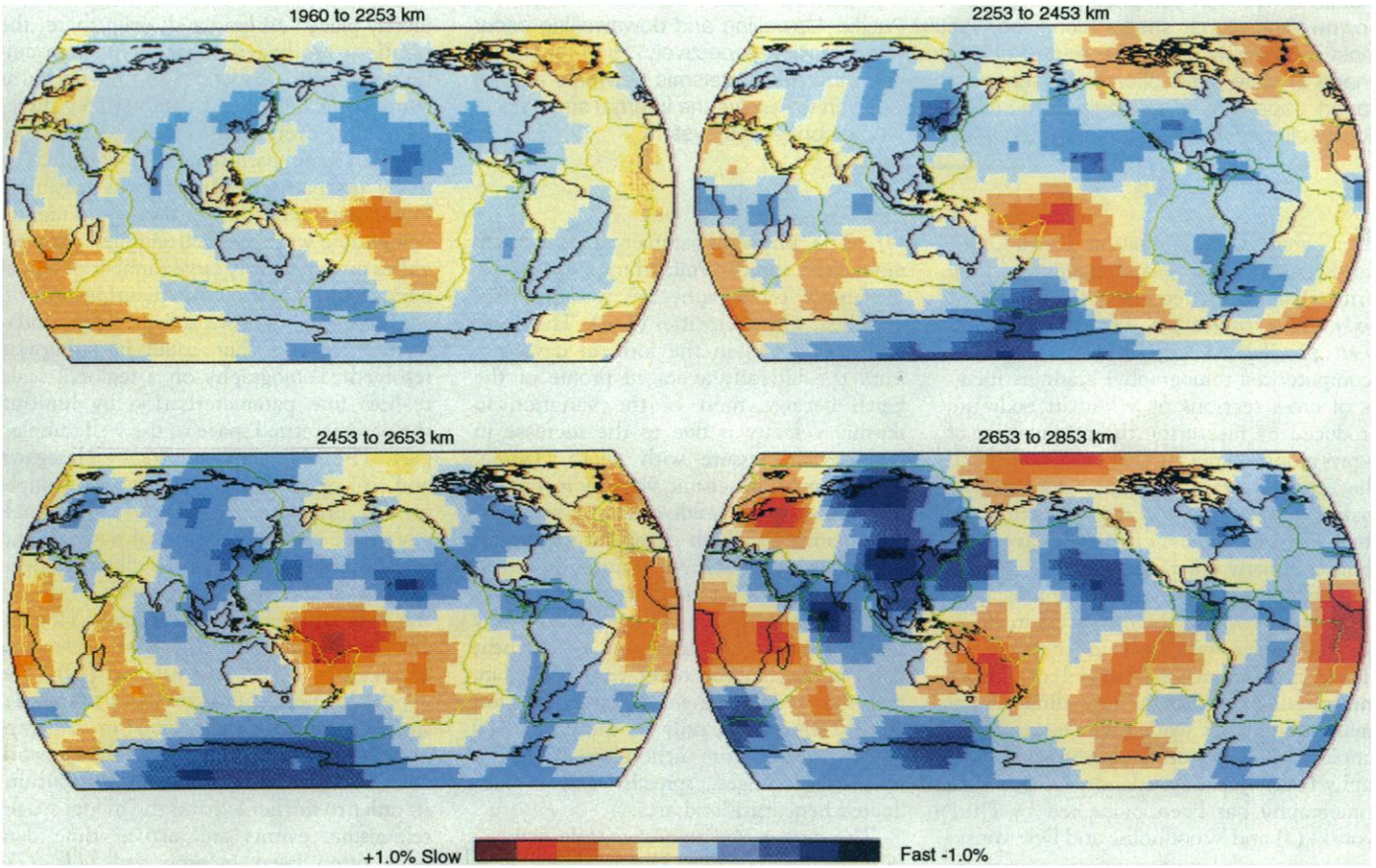

Fig. 2. Smoothed seismic velocity perturbations maps of four layers in a depth range 38 to 931 km above the CMB. The scale ranges from −1% (blue) to +1% (red).

obtained in the earlier step.

Figure 1 shows a great circle cross section of velocity anomalies in the mantle. The outermost ring is closest to the Earth's surface, the innermost corresponds to the core-mantle boundary (CMB) at a depth of 2900 km. This figure (faster region in blue and slower region in red) is a composite diagram of the unsmoothed section beneath the west Pacific (maximum velocity contrast: ±2%) and the smoothed section in the rest of the mantle (maximum contrast: ±1%). This figure illustrates the strategy to focus on the Japanese islands as a part of the west Pacific and the west Pacific as a part of the whole Earth. More specifically, this figure illuminates the main targets of my discussion: the downwelling current under the west Pacific and the upwelling current under the south Pacific. The former is imaged as a slab-like fast anomaly plunging downward from the Bonin trench and lying under the Philippine Sea. The upwelling current is imaged as a low-velocity column rising from the CMB through the lower mantle toward the area of the Polynesian hot spots (active intraplate volcanoes). A high-velocity image of oceanic plates about 100-km thick is hardly seen because the oceanic upper mantle is poorly resolved in P-wave tomography (see Fig. 3).

Slabs in the transition zone. As shown in Fig. 1, the high-velocity pattern, presumably marking the slab, dips steeply from the Bonin trench and then bends sharply to subhorizontal. The steeply dipping portion delineates the Wadati-Benioff seismic zone (*13*). The aseismic subhorizontal part is 2000 km long, but this length results because the projection of the figure is oblique to the trench system; the length in a direction perpendicular to the trench is approximately 1000 km. The subhorizontal part of the slab from the Izu-Bonin trench lies above the 660-km discontinuity. Okino *et al.* (*14*) were the first to recognize this remarkable feature, which has been later confirmed by tomographic studies (*12*, *13*, *15*). The horizontal slab image from the Japan trench, on the other hand, apparently thickens vertically so that its bottom is located in the lower mantle well below the 660-km discontinuity (*13*). Under the Java arc, on the other hand, the image of high velocity slab appears to dip steeply and to penetrate the 660-km discontinuity, it then immediately bends to a shallow dip with a considerable vertical spread, reaching a depth of about 1200 km (*13*). A similar image has also been obtained for the northern Kurile arc (*15*). Although resolution beneath other island arcs in the west Pacific is not as high as for the above arcs, the transition zone beneath them is commonly dominated by a fast anomaly (*16*, *18*). On the basis of these results Fukao *et al.* (*13*) suggested that descending slabs of lithosphere in the west Pacific tend to stall in the transition zone under a subtle control of the 660-km discontinuity, although it appears that a substantial amount of slab materials eventually sinks into the lower mantle. The more recent whole-mantle tomography of S-wave velocities (*8*) seems to support this concept of slab stagnation, which is an alternative to the idea of slab penetration (*16*).

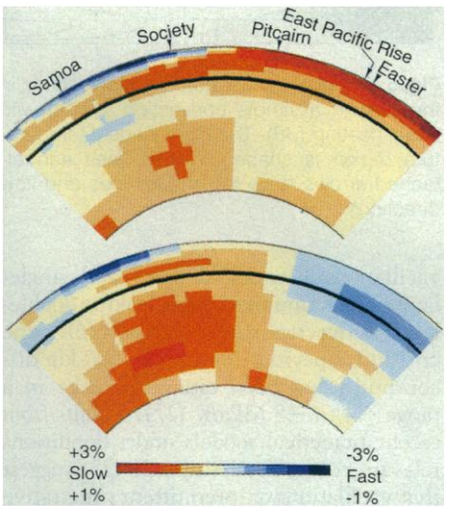

Fig. 3. A cross section of seismic velocity perturbations in the mantle along a great circle with a pole at (65°N, 105°W). This cross section is approximately parallel to the traces of the Polynesian hot spots. Arrows indicate the approximate locations of some of the hot spots and the East Pacific Rise. The boundary between the upper and lower mantle at a depth of 660 km is shown by a solid black line. (**A**) A discretized version of SH8/WM13 (*16*), for which the S-wave perturbation ranges from −3% (blue) to +3% (red). The slow anomaly under the East Pacific Rise and Easter Island exceeds 3%. (**B**) P-wave velocity perturbations, from −1% (blue) to +1% (red), from (*13*).

Pacific superplume. The low-velocity column beneath the south Pacific (Fig. 1) has a tapered shape that is broadest at the base of the mantle, where the resolution is relatively poor. To obtain a sharper image of this tapered shape, Obayashi *et al.* (*17*) did an inversion by including in the arrival time data of the PcP wave (a P wave once reflected at the CMB). The PcP data were not corrected for the possible effect of topography on the CMB (*18*). Rather the effect was absorbed into the velocity perturbation of the bottom 40-km-thick layer, which is poorly sampled by the first-arrival data. This treatment is similar to the way of handling a structural anomaly near the receiver, the effect of which is absorbed into the velocity perturbation of the top 30-km-thick layer (the crustal layer). The velocity anomalies of the top and bottom layers may therefore be distorted and are not discussed further.

Two features first discovered by Dziewonski (*3*) are evident also in the results with the PcP data (Fig. 2): (i) the low-velocity column under the south Pacific and (ii) the high-velocity sheet around the Pacific. Note that the lowermost mantle under Hawaii (an active hot spot) is fast. The addition of the PcP data little changed the overall pattern of heterogeneity but increased the magnitude and resolution of the south Pacific slow anomaly in the D″ layer (the bottom 200- to 300-km-thick layer of the mantle). As shown in Fig. 2, the south Pacific slow anomaly progressively broadens with depth mainly to the east and west within 500 to 600 km of the CMB. In the D″ layer this anomaly is apparently separated into the east and west parts with a near-zero anomaly in between. Such a separation, however, may be a spurious because of the lack of resolution: the central part could be equally anomalous (*17*). Within a thickness of 1000 km above the CMB, the intensity of overall heterogeneity progressively increases with depth (from ±0.5 to ±1.0%). Such an increase is already apparent in the early model of Dziewonski (*3*), and the addition of PcP data simply substantiated the highest intensity in the D″ layer.

The south Pacific slow anomaly rises as a relatively narrow column at depths above 2300 km. At depths shallower than 1400 km it spreads to the north to apparently include Hawaii and to the south to apparently include the Louisville Ridge and Mt. Erevus (*17*). The resolution is not good enough to trace the continuation in the upper mantle in detail. Better resolution of this region is available in a recent S-wave velocity model, SH8/WM13 (*8*), which was obtained from waveform data of surface waves and surface-reflected S waves. Figure 3A shows a cross section of this model under the south Pacific. This profile is taken to be approximately parallel to the tracks of the Polynesian hot spots, which define the major axis of the anomalous topographic high (250 to 1000 m shallower than normal) in a broad area of French Polynesia (18 million square kilometers); McNutt and Fisher (*19*) termed this region the South Pacific superswell. Figure 3B shows the corresponding cross section of the P-wave velocity model (*13*) (note the scale is different between the two models). Under Tahiti (Society islands), the two models consistently show a large body of slow anomaly rising from the CMB which images the present-day Pacific superplume (*20*) (an extraordinary upwelling of heat and deep-mantle material in the form of one or several very large plumes). This slow anomaly apparently continues into the upper mantle with some intermission near

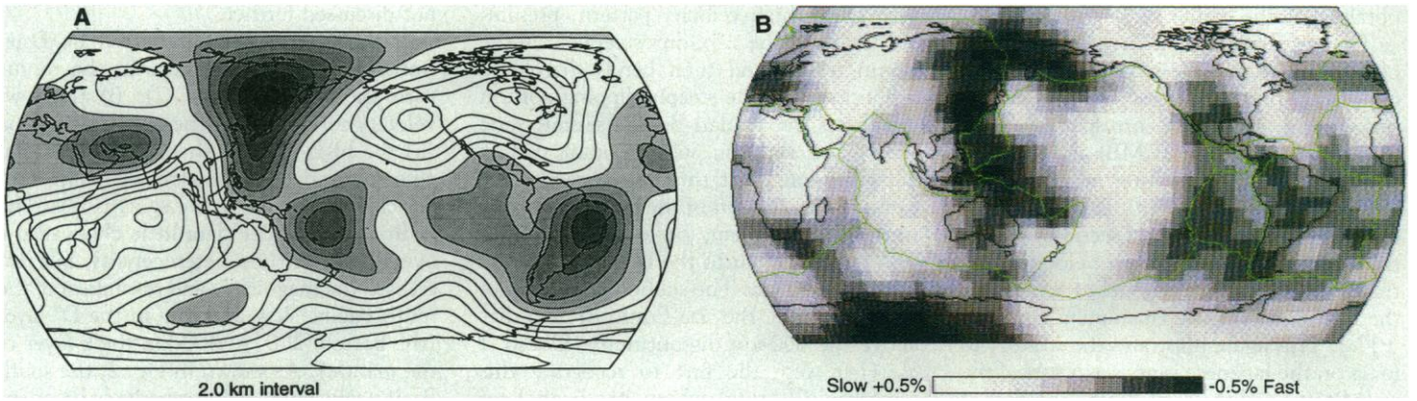

Fig. 4. Comparison between the topography on the 660-km discontinuity (**A**) and the slowness perturbation of the layer in a depth range from 629 to 800 km (**B**). The topography is contoured at an interval of 2 km and the region of depression is shaded (*21*). The scale ranges from −0.5% (black) to +0.5% (white). The scale saturates locally.

the top of the lower mantle. The upper mantle part of slow anomaly, under Tahiti, is capped by a high-velocity lid which perhaps marks the oceanic plate of lithosphere. In Fig. 3A, this upper mantle slow anomaly is subhorizontally connected to one just beneath the East Pacific Rise, a feature unresolvable from P-wave tomography (Fig. 3B).

Topography on the 660-km discontinuity. The nature of the boundary between the upper and lower mantle is revealed by comparing (Fig. 4) the smooth I-wave velocity perturbation map in the vicinity of the 660-km discontinuity (*13*) to the smooth topography map of the 660-km discontinuity obtained by the analysis of long-period SS waves (*21*). The velocity perturbation is on the order of ±0.5%, whereas the boundary undulation is on the order of ±10 km around a mean depth of 660 km. The boundary is most depressed in the west Pacific, where the velocity perturbation is highest. Such a correlation between the boundary depression and a positive velocity perturbation is persistent throughout the region of subduction in the west Pacific from Kamchatka to Kurile, Japan, the Philippines, New Guinea, New Hebrides, and west of Tonga. The antipodal region, South America, is also marked by a fast anomaly and depression of the boundary. On the other hand, the 660-km discontinuity is generally shallow beneath North America, Antarctica, and the Indian Ocean, where the mantle near the 660-km discontinuity is consistently slow. Thus there is a good correspondence in large-scale pattern between the velocity anomaly near the 660-km discontinuity and its undulation, although the correspondence is admittedly not perfect.

According to the results of high-pressure experiments, magnesium-rich olivine, $(Mg,Fe)_2SiO_4$, the most abundant mineral in the upper mantle, transforms at a depth corresponding to the 660-km discontinuity from the spinel structure to a mixture of magnesiowustite $(Mg,Fe)O$ and pyroxene $(Mg,Fe)SiO_3$ in the perovskite structure (*22*). This reaction is endothermic and has a negative Clapeyron slope of about −2 to −4 MPa/K (*22*) so that the phase boundary would move downward in the low-temperature (thus high-velocity) region. If the 660-km discontinuity is such a phase boundary, the observed smooth topography of ±10 km would be explained by a temperature perturbation of the order of ±100 K, which corresponds to a velocity perturbation of the order of ±1%, in fair agreement with the observed perturbation of ±0.5%. A more direct comparison based on the unsmoothed results is possible in the northwest Pacific subduction zones, where a depression of the discontinuity of 5 to 10, 15 to 20, and 20 to 30 km has been reported from the analysis of long-period ScS waves (*23*), long-period SS waves (*21*) and short-period SP waves (*24*), respectively. The depression of this magnitude would be explained by a temperature decrease of 50 to 300 K, which corresponds to a velocity increase of 0.5 to 3%, in fair agreement with the observed slab-like fast anomaly of 2% at depths near the 660-km discontinuity (Fig. 1). This agreement strongly supports hypothesis that the 660-km discontinuity is a phase boundary, but it does not preclude the possibility of compositional change in addition to the pressure-induced phase transition, because the expected compositional change is unlikely to accompany an appreciable velocity change (*25*).

Implications for Mantle Convection

Numerical calculations of mantle convection indicate that although the endothermic nature of the 660-km discontinuity impedes slab penetration, a slab can still penetrate the lower mantle if the Clapeyron slope is above a critical value (*26*). For a Clapeyron slope near the critical value,

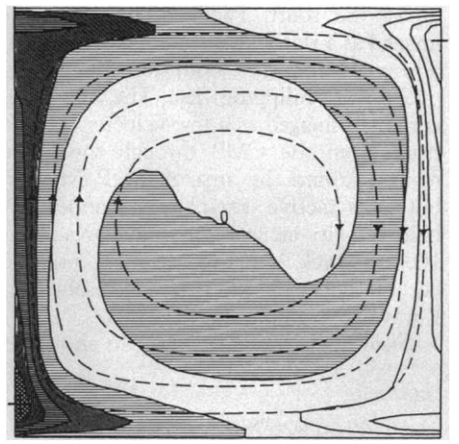

Fig. 5. Residual temperature field (as defined in the text) in a simple convection system with basal heating (*36*). The high residual temperature region is shaded. Dotted lines and attached arrows show the stream lines and flow directions.

vacillations between double- and single-layer convection or strongly leaking double-layer convection are possible (*26*). The critical Clapeyron slope at the 660-km discontinuity has been estimated to be in a range −4 to −8 MPa/K (*27*). Results from recent numerical models under conditions relevant to the Earth's mantle (*28*) suggest that vacillations or intermittent penetrative convection can occur for much smaller endothermic Clapeyron slopes that are compatible with the experimentally reported values in a range −2 to −4 MPa/K (*22*). Such convection near the critical state appears to be consistent with the recent tomographic image of slab stagnation in a variety of form, from almost complete deflection of a subducted slab at the base of the upper mantle to almost direct sinking into the lower mantle (*13, 15*). The chemical heterogeneity of subducted slabs (*29*), possible compositional change across the 660-km discontinuity (*25, 26*) and occur-

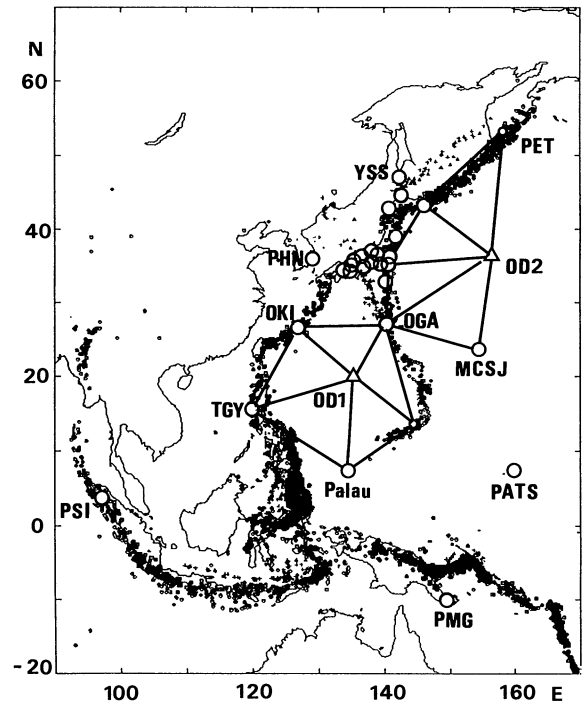

Fig. 6. Present status of the pre-POSEIDON Network (large open circles). There are now 17 stations on the main Japanese islands. Other currently active stations are OKI (Ryukyu), OGA (Bonin), MCSJ (Marcus), PHN (Korea), TGY (Luzon), PSI (Sumatra) and YSS (Sakhalin: IRIS-POSEIDON). PATS (Pohnpei) is under construction. Stations on Palau and PMG (Papua New Guinea) are being planned. Small open circles are the IRIS stations, GUA (existing) and PET (under construction). Triangles are the two ODP sites proposed in conjunction with the pre-POSEIDON project. These sites are shown to be tied to the surrounding subareal stations to demonstrate the role of emplacement of only one or two ODP downhole seismometers for a uniform station coverage on the ocean bottom. The smaller dots are earthquakes deeper than 50 km.

rence of multiple phase transitions (*30*) may also contribute to the various forms of slab stagnation.

As shown in Fig. 2, the Circum Pacific fast anomaly at the base of the mantle is at a maximum under East Eurasia, in good geographical correspondence with the fastest anomaly at the transition zone (Fig. 3; see also Fig. 1). This maximum anomaly under East Eurasia is sharply confined within the D″ layer and does not extend to shallower layers. It is intriguing that the PdP phase (a P phase once reflected at the top of the D″ layer) has been so far most convincingly reported in this region (*31, 32*), that is, the top of the D″ layer is sharp in terms of P wave velocity in this region. PdP studies in other regions show that such a sharp boundary is not a global feature (*31*). The geographical correspondence of the fastest anomaly between the transition zone and the D″ layer may imply that a downwelling current is developed from the top to bottom of the lower mantle most extensively in this region. The fastest anomaly of +1% in the D″ layer appears to be too large to be explained only by a thermal boundary layer; thus, some compositional variation seems to be required (*33*). The observed sharp velocity contrast at the top of the D″ layer also requires that either a phase or compositional change be present (*32*). Thus, the D″ layer may be chemically distinct from the rest of the lower mantle (*34*), and intrusion of cold downwelling mantle into this layer may involve some type of phase change and produce some lateral compositional variation (*35*), although these possibilities remain speculative.

Further implications for the processes occurring in the D″ layer may be obtained by comparing the seismic tomographic results with the residual temperature field $\delta T = T - \langle T \rangle$ of simple thermal convection experiments (Fig. 5) with a high Rayleigh number ($Ra = 3 \times 10^5$), where $\langle T \rangle$ is the horizontally averaged temperature profile (*36*). The hot plume on the left side of the convection cell in Fig. 5 arises from the thermal boundary layer at the bottom, where the high-temperature residual anomaly elongates to horizontal. This elongation may be compared to the extensive horizontal spread of the south Pacific slow anomaly in the lowermost mantle (Fig. 2). Such apparent similarity seems to imply that the present-day Pacific superplume has its origin in the D″ layer that acts as a thermal boundary layer. The horizontal spread of slow anomaly should also be observed, if a chemical layer coexists with the thermal boundary layer at the CMB (*35, 37*).

The combination of rising columnar plumes and sinking tabular sheets is a fundamental property of convection in a viscous spherical shell with some basal heating (*38*). The sinking sheets near the surface are lithospheric plates themselves subducting from deep-sea trenches around the Pacific. One of the rising plumes would be the present-day Pacific superplume marked by the south Pacific slow anomaly. The results in Fig. 3A seem to imply that this rising plume is prevented from outpouring onto the surface by the overlying oceanic plate; instead, it finds its way out at the East Pacific Rise, where there is a gap between the two plates. The superswell of French Polynesia (*19*) and its extensive hot-spot volcanism (*39*) may then be understood as a thermal and mechanical response of the plate to the rising current associated with the superplume.

In Fig. 3 (both A and B), the south Pacific slow anomaly in the lower mantle continues to the upper mantle with some intermission directly below or near the 660-km discontinuity. The absence of strong anomaly in this depth range is also clear not only in the velocity perturbation map (Fig. 4B) but also in the topography map of the 660-km discontinuity (Fig. 4A). This absence may be compared to the absence of strong anomaly in the residual temperature field for the upwelling plume just below the upper thermal boundary layer in the convection experiment (Fig. 5). Alternatively, the absence may imply an interaction of the superplume with the 660-km discontinuity (*40*). At present, the mechanism and extent of mass transfer from the lower to upper mantle are even more obscure than one from the upper to lower mantle in the subduction zones.

Future Progress

The above is a global image of mantle circulation in the Pacific hemisphere yielded by applications of seismic tomography. Two key regions in this image are the south Pacific as a place of mantle upwelling and the west Pacific as a place of downwelling. Further advances will rely more on regional-scale tomographic experiments through installation of a large number of high-quality instruments in these regions. Results of such experiments have to be eventually integrated into a global image with the aid of worldwide seismic networks to understand the processes occurring under the target regions as integral parts of mantle convection. It is straightforward to go one step further, especially in the west Pacific where dense networks are available in some island arcs. For example, the high-resolution image of plate subduction beneath Japan (*9, 10*) can in principle be integrated into a broader image of mantle downwelling under the west Pacific. The progress in this direction, however, requires a reorganization of the observation system such that seismic activity in the Japanese islands can be monitored as a part of the activity in the west Pacific and the latter as a part of the whole Earth activity. Under Japan's earthquake prediction program, the main Japanese islands are now covered with dense seismograph networks operated by the Japan Meteorological Agency (JMA), the National Research Institute for Earth Sciences and Disaster Prevention (NIED) and the national universities with their mutual

linkage. On one hand, worldwide high-quality networks, such as GEOSCOPE (*41*) and IRIS (*42*), are now at least in part in routine operation. Thus, the reorganization of the observation system can be accomplished, in principle, by developing a seismograph network comparable in size to the west Pacific; this network could serve as a link between the Japanese networks and the global networks.

There have been continuing efforts to set up broadband seismographs in the west Pacific, mostly on the Japanese islands but also elsewhere, as illustrated in Fig. 6 (*43*). Integration of these seismograph stations is intended to be a preliminary version (pre-POSEIDON) of the proposed POSEIDON network (Pacific Orient Seismic Digital Observation Network). Because there are only a few land areas in the west Pacific, uniform station coverage is extremely difficult without a complement of ocean bottom seismographs (OBS). As shown by Kanazawa *et al.* (*44*), digital and broadband sensors can be placed in drill holes to record seismic tremors at nearby and teleseismic distances. A key element of the pre-POSEIDON project is installation of a few ODP (Ocean Drilling Project) downhole stations and their linkage to the subareal stations. As shown in Fig. 6 emplacement of only one or two ODP downhole seismometers can provide good station coverage for the network. Obviously it is impossible to obtain a global image of mantle convection from the Japanese network data alone. Likewise it is impossible to obtain a sharp image of plate subduction only from the global network data. Linkage of the west Pacific network (POSEIDON) to the Japanese networks and the global networks will bring a favorable interaction among different scales, thus yielding a less biased image of plate subduction and mantle downwelling in the west Pacific and at the same time a more comprehensive image of mantle convection. Similar interaction should be expected in many fields of seismology including earthquake prediction research.

REFERENCES AND NOTES

1. K. Aki, A. Christofferson, E. S. Husebye, C. Powell, *Eos* **56**, 1145 (1974).
2. K. Hirahara, *J. Phys. Earth* **25**, 393 (1977).
3. A. M. Dziewonski, *J. Geophys. Res.* **89**, 5929 (1984).
4. J. H. Woodhouse and A. M. Dziewonski, *ibid.*, p. 5953; see also A. M. Dziewonski and J. H. Woodhouse, *Science* **236**, 37 (1987).
5. P. Olson, P. G. Silver, R. W. Carlson, *Nature* **344**, 209 (1990).
6. F. M. Richter, *J. Geophys. Res.* **84**, 6783 (1979).
7. B. H. Hager, *ibid.* **89**, 6003 (1984); B. H. Hager, R. W. Clayton, M. A. Richards, R. P. Comer, A. M. Dziewonski, *Nature* **313**, 541 (1985).
8. R. L. Woodward, A. M. Forte, W. Su, A. M. Dziewonski, in *Chemical Evolution of the Earth and Planets*, R. Jeanloz and E. Takahashi, Eds. (*Geophys. Monogr.*, American Geophysical Union, Washington, DC, in press).
9. A. Hasegawa, D. Zhao, S. Hori, A. Yamamoto, S. Horiuchi, *Nature* **352**, 683 (1991); D. Zhau, A. Hasegawa, S. Horiuchi, *J. Geophys. Res.*, in press.
10. See for the Hokkaido arc, H. Miyamachi and T. Moriya, *J. Phys. Earth* **32**, 13 (1984), and for the central Honshu arc, M. Ishida and A. Hasemi, *J. Geophys. Res.* **93**, 2076 (1988); K. Hirahara, A. Ikami, M. Ishida, T. Mikumo, *Tectonophysics* **163**, 63 (1989).
11. S. Kamiya, T. Miyatake, K. Hirahara, *Geophys. Res. Lett.* **15**, 828 (1988); *Bull. Earthq. Res. Inst. Univ. Tokyo* **64**, 457 (1989).
12. H. Zhou and R. W. Clayton, *J. Geophys. Res.* **95**, 6829 (1990).
13. Y Fukao, M. Obayashi, H. Inoue, M. Nenbai, *ibid.* **97**, 4809 (1992); see also H. Inoue, Y. Fukao, K. Tanabe, Y. Ogata, *Phys. Earth Planet. Inter.* **59**, 294 (1990).
14. K. Okino, M. Ando, S. Kaneshima, K. Hirahara, *Geophys. Res. Lett.* **16**, 1059 (1989).
15. R. van der Hilst, R. Engdahl, W. Spakman, G. Nolet, *Nature* **353**, 37 (1991).
16. T. H. Jordan, *J. Geophys. Res.* **83**, 473 (1977); K. C. Creager and T. H. Jordan, *ibid.* **89**, 3031 (1984); *ibid.* **91**, 3573 (1986).
17. M. Obayashi, Y. Fukao, H. Inoue, paper presented at the 3rd Study of the Earth's Deep Interior (SEDI) Symposium, Mizusawa, July 1992.
18. K. C. Creager and T. H. Jordon, *Geophys. Res. Lett.* **13**, 1497 (1986); A. Morelli and A. M. Dziewonski, *Nature* **325**, 678 (1987); D. J. Doornbos and T. Hilton, *J. Geophys. Res.* **94**, 15741 (1989).
19. M. K. McNutt and K. Fischer, in *Seamounts, Islands, and Atolls*, B. H. Keating, P. Fryer, R. Batiza, G. W. Boehlert, Eds. (*Geophys. Monogr. 43*, American Geophysical Union, Washington, DC, 1987), p. 25; see also M. K. McNutt and A. V. Judge, *Science* **248**, 969 (1990).
20 R L Larson, *Geology* **19**, 547 (1991); *ibid.*, p. 963.
21 P. M. Shearer and T. G. Masters, *Nature* **355**, 791 (1992).
22. E. Ito and H. Yamada, in *High-Pressure Research in Mineral Physics*, S. Akimoto and M. H. Manghnani, Eds. (Center for Academic Publications, Tokyo, 1982), p. 405; E. Ito and E. Takahashi, *J. Geophys. Res.* **94**, 10637 (1989); E. Ito, M. Akaogi, L. Topor, A. Navrotsky, *Science* **249**, 1275 (1990).
23. J. Revenaugh and T. H. Jordan, *J. Geophys. Res.* **94**, 5787 (1989).
24. J. E. Vidale and H. M. Benz, *Nature* **356**, 678 (1992).
25. R. Jeanloz, *Geophys. Res. Lett.* **18**, 1743 (1991).
26. U. R. Christensen and D. A. Yuen, *J. Geophys. Res.* **89**, 4389 (1984); U. R. Christensen, in *Mantle Convection*, vol. 4 of *The Fluid Mechanics of Astrophysics and Geophysics*, W. R. Peltier, Ed. (Gordon and Breach, New York, 1989), p. 595.
27. U. R. Christensen and D. A. Yuen, *J. Geophys. Res.* **90**, 10291 (1985).
28. P. Machetel and P. Weber, *Nature* **350**, 55 (1991).
29. A. E. Ringwood and T. Irifune, *ibid.* **331**, 131 (1986), U. R. Christensen, *ibid.* **336**, 462 (1988).
30. W. Zhao, D. A. Yuen, S. Honda, *Phys. Earth Planet. Inter.* **72**, 185 (1992).
31. M. Weber and J. P. Davis, *Geophys. J. Int.* **102**, 231 (1990).
32. S. Houard and H. Nataf, *Phys. Earth. Planet. Inter.* **72**, 264 (1992).
33. F. D. Stacy, paper presented at the 3rd SEDI symposium, Mizusawa, July 1992.
34. P. G. Silver, R. W. Carlson, P. Olson, *Annu. Rev. Earth Planet. Sci.* **10**, 477 (1988); E. Knittle and R. Jeanloz, *Geophys. Res. Lett.* **16**, 609 (1989).
35. G. F. Davies and M. Curnis, *Geophys. Res. Lett.* **13**, 1517 (1986); U. Hansen and D. A. Yuen, *ibid.* **16**, 629 (1989).
36. S. Honda, *J. Phys. Earth* **35**, 195 (1987).
37. N. H. Sleep, *Geophys. J.* **95**, 437 (1988).
38. D. Bercovici, G. Schubert, G. A. Glatzmaier, *Science* **244**, 950 (1989); *Geophys. Res. Lett.* **16**, 617 (1989).
39. D. L. Tumer and J. R. Jarrard, *J. Volcanol. Geotherm. Res.* **12**, 187 (1982); R. A. Duncan and D. A. Clague, in *Ocean Basins and Margins*, A. E. M. Naim, F. G. Stehli, S. Uyeda, Eds. (Plenum, New York, 1985), p. 89.
40. L. H. Kellogg, *Geophys. Res. Lett.* **18**, 865 (1991).
41. B. Romanowicz *et al.*, *Bull. Seismol. Soc. Am.* **81**, 243 (1991).
42. S. W. Smith, *Eos* **67**, 213 (1986); IRIS (Incorporated Research Institutions for Seismology), in *FDSN* (Federation of Digital Broadband Seismograph Networks) *Netw. Rep.* (August 1991).
43. POSEIDON, in *ibid.*
44. T. Kanazawa, K. Suyehiro, N. Hirata, M. Shinohara, *Proc. Ocean Drill. Proj. SR 127/128*, in press; K. Suychiro, T. Kanazawa, N. Hirata, M. Shinohara, H. Kinoshita, *ibid.*, *SR 127/128*, in press.
45. Some of the tomographic results are from my paper in preparation with M. Obayashi and H. Inoue (*17*). I thank two anonymous reviewers for many invaluable comments. This work was in part supported by the Grant-in-Aid for Scientific Research (no. 03232101) from the Japanese Ministry of Education.